

Analysis of a Microstrip Line Terminated with a Shorting Pin

Wen-Jiunn Tsay and James T. Aberle

Abstract—A full-wave moment method solution to the problem of a semi-infinite microstrip line terminated with a shorting pin is presented. The electric current on the line is expanded in terms of longitudinal piecewise sinusoidal modes near the open end, with entire domain traveling-wave modes to represent incident and reflected waves away from the open end. Also, the electric current near the shorting pin is simulated by an attachment mode which insures continuity of the current between the pin and the line and models the rapidly-varying current on the line near the feed connection point. Results are given for the magnitude of the reflection coefficient and are compared with experimental data.

I. INTRODUCTION

BECAUSE of its easy mounting capabilities and inexpensive fabrication processes, microstrip line is the most often selected transmission medium for use in microwave and millimeter-wave integrated circuit applications.

Discontinuities in the microstrip line are frequently used as circuit elements in device design. Because these discontinuities are rarely amenable to closed-form solution, some level of modeling must be used in their design and analysis. The simplest and most computationally efficient models use quasi-static techniques to describe the discontinuities in terms of equivalent lumped-element circuits. Such models are used in many computer-aided design (CAD) packages. However, these simple models are often inadequate for use in the design of many advanced systems, because they fail to account fully for the electromagnetic effects of the discontinuities.

In many cases, it is uneconomical or impossible to fine-tune the circuit once it has been fabricated. As a result, circuit designers are forced to perform a costly iterative cut-and-try stage in the design. Thus, there has been a great deal of interest in more accurate treatments of microstrip discontinuities [1]–[7]. Because many of these more rigorous solutions require large amounts of computer time and memory, they have to date been considered unattractive candidates for use in a CAD package. However, recent advances in the capabilities of engineering

Manuscript received June 17, 1991; revised October 24, 1991. This work was supported in part by Arizona State University Faculty-Grant-In-Aid and by the Telecommunications Research Center.

W.-J. Tsay is with the Department of Electrical and Computer Engineering, University of Massachusetts, P.O. Box 2681, Amherst, MA 01002.

J. T. Aberle is with the Telecommunications Research Center, Arizona State University, Tempe, AZ 85283.

IEEE Log Number 9106040.

workstations and supercomputers are helping to alleviate this situation. In the near future, we can expect significant improvements in this area.

Because of significant advantages over the method of lines [7]–[8] and the finite difference method [4]–[6], the integral equation technique [9]–[16] is the best approach for the investigation of microstrip discontinuities. The most appropriate method for obtaining the integral equation description of the problem under consideration is the spectral domain approach [11], [12], [18]. Formulation of the problem is facilitated in the spectral domain since the Green's function for the planar structure is given in closed-form. While variational solutions for the integral equations have been obtained [9], better accuracy can be obtained using the moment method.

Numerical models for the discontinuities studied here have been developed using the spectral domain approach to obtain an electric field integral equation (EFIE) description of the problem. The EFIE is discretized using the moment method, and the resulting matrix equations are solved on the computer.

The solution presented here represents an attempt to extend the theory of [12] to the case of a microstrip line terminated with a shorting pin. At lower frequencies, the theoretical and experimental results closely agree with each other. But, error can be as large as 30% at higher frequencies. We attribute these errors at higher frequencies mainly to the neglect of the transverse current component. More work is needed to overcome this deficiency.

II. THEORY

Consider a semi-infinite microstrip line with a shorting pin connected to the ground plane in the vicinity of the open end, as shown in Fig. 1. The ground plane, microstrip line and shorting pin are all assumed to comprise perfect electric conductor, and the substrate is assumed to be infinite in the x - and y -directions. The substrate is of thickness d which is assumed to be very thin such that only the fundamental mode can propagate in the microstrip line. The upper conductor has width w . The pin connection point is located at $(x, y) = (x_p, y_p)$, and the radius of the pin is r_o , which is assumed to be much smaller than the effective wavelength.

The full-wave solution for this problem developed here requires 1) the infinite grounded dielectric slab dyadic Green's function for the electric field due to an electric

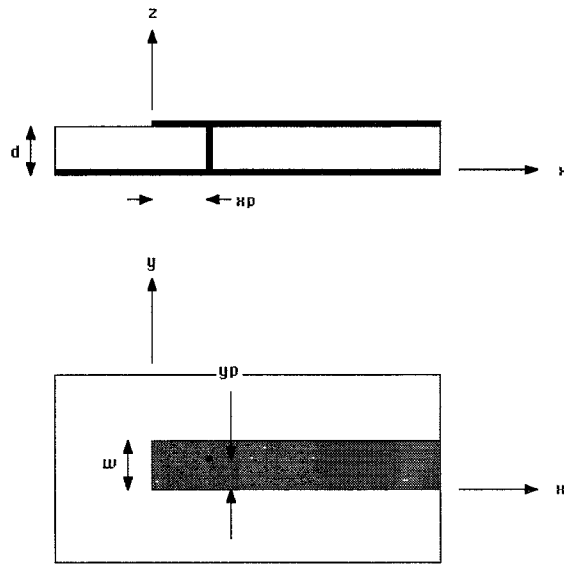


Fig. 1. Open-end microstrip line terminated with a shorting pin.

current distribution, 2) the effective propagation constant of an infinitely long microstrip line, and 3) current expansion modes that can accurately account for the natural current behavior of the structure. We set up an integral equation description of the boundary condition that the tangential electric field must vanish on the microstrip line and the shorting pin, and expand the unknown current in a suitable set of basis functions. By following Galerkin's procedure, we can determine the unknown current and, thus, the voltage reflection coefficient of the discontinuity. This solution is "full-wave" because all of the electromagnetic features of the problem such as surface wave and radiation effects are included in the solution since the exact Green's function for the structure is used.

The dyadic Green's function for the electric field due to an electric current distribution in and on a grounded dielectric slab is well-known in both spatial and spectral domain forms. In this paper, the spectral domain form is used.

In dyadic form, the Green's function can be written as

$$\begin{aligned} \bar{E} = & \hat{x}E_{xx}\hat{x} + \hat{x}E_{xy}\hat{y} + \hat{x}E_{xz}\hat{z} + \hat{y}E_{yx}\hat{x} + \hat{y}E_{yy}\hat{y} \\ & + \hat{y}E_{yz}\hat{z} + \hat{z}E_{zx}\hat{x} + \hat{z}E_{zy}\hat{y} + \hat{z}E_{zz}\hat{z} \end{aligned} \quad (1)$$

where

$$\begin{aligned} E_{pq}(x, y, z | x_o, y_o, z_o) = & \frac{1}{4\pi^2} \int_{-\infty}^{\infty} \int_{-\infty}^{\infty} G_{pq}(k_x, k_y, z | z_o) \\ & \cdot e^{jk_x(x-x_o)} e^{jk_y(y-y_o)} dk_x dk_y \end{aligned} \quad (2)$$

and $E_{pq}(x, y, z | x_o, y_o, z_o)$ is the \hat{p} -directed electric field at the point (x, y, z) due to an infinitesimal \hat{q} -directed current element at (x_o, y_o, z_o) . The G_{pq} 's required in this analysis are given in the Appendix.

The effective propagation constant of an infinitely long microstrip line is also required for this analysis and may be obtained using the full-wave technique described in [12]. The method of solution involves expanding the electric current density on the microstrip line and on the shorting pin, then formulating an electric field integral equation (EFIE) which can be solved by the method of moments for the reflection coefficient and the unknown expansion currents. The choice of basis functions affects the computational efficiency quite significantly, so a judicious choice is important.

Because of the complicated discontinuous nature of the current on the microstrip line near the pin attachment point, it is very difficult to accurately describe the current behavior of this discontinuity using simple basis functions. The approach used here is similar to the one used in [18].

There are three kinds of basis functions used here, which are the sinusoidal modes, the piecewise sinusoidal (PWS) modes, and the attachment mode. Fig. 2 qualitatively illustrates these modes. For sinusoidal and piecewise sinusoidal modes, the current distribution in the y -direction is assumed to be Maxwellian.

Since we assume only the fundamental microstrip mode can propagate down the line when it is away from the open end and the shorting pin, it is reasonable to use sinusoidal functions to represent incident and reflected traveling waves of the fundamental microstrip mode. Subsectional (piecewise sinusoidal) modes are used near the open end to represent currents that do not conform to the fundamental mode as in [12]. These basis functions together with their Fourier transforms (required for the spectral domain analysis) are described in detail in [12].

A critical component of our solution is the use of a suitable basis function which can insure continuity of current from the microstrip line to the shorting pin and model the rapidly-varying surface current near the pin connection point. The method used to generate this attachment mode is similar to [18].

Because the line is semi-infinite, it is assumed that the part of the attachment mode on the microstrip line only exists between $x = 0$ and $x = L_1$. Using this assumption, we can obtain an equivalent model for generating an attachment mode with the desired properties. The equivalent model is shown in Fig. 3, and consists of a uniform current probe exciting a rectangular cavity comprising perfect electric conductor on top and bottom and perfect magnetic conductor around the sides. Since d is very thin we can assume that there is no z -variation and only TM_z modes can exist inside the structure. This equivalent model can be treated as a traditional boundary value problem.

Solving for the surface current density on the upper conductor, we obtain

$$\vec{J}_{ax}(x, y) = \frac{1}{2w} \sum_{n=0}^{\infty} \epsilon_n \cos\left(\frac{n\pi}{w} y_p\right) \cos\left(\frac{n\pi}{w} y\right) \frac{\sin[\beta_{xn}(L_1 - x - x_p)] + \operatorname{sgn}(x - x_p) \sin[\beta_{xn}(L_1 - |x - x_p|)]}{\sin(\beta_{xn} L_1)} \quad (3)$$

where

$$\text{sgn}(t) = \begin{cases} 1, & \text{if } t > 0 \\ -1, & \text{if } t < 0 \end{cases}. \quad (4)$$

$$\vec{J}_{ay}(x, y) = \frac{-1}{w} \sum_{n=1}^{\infty} \frac{n\pi}{w} \cos\left(\frac{n\pi}{w} y_p\right) \sin\left(\frac{n\pi}{w} y\right) \frac{\cos[\beta_{xn}(L1 - x - x_p)] + \cos[\beta_{xn}(L1 - |x - x_p|)]}{\beta_{xn} \sin(\beta_{xn} L1)}. \quad (5)$$

The z component of the attachment mode exists on the pin and is given by

$$\vec{J}_{az}(x, y) = \hat{z} \delta(x - x_p) \delta(y - y_p). \quad (6)$$

The attachment mode basis function described by (3), (5), and (6) exhibits proper behavior near the pin connection point and enforces continuity of current (through the end-charge cancellation concept) from the pin to the line.

The unknown current distribution on the line and the pin is expanded as

$$\begin{aligned} \vec{J}(x_o, y_o, z_o) &= \hat{x} [J_{\text{inc}}(x_o, y_o) + J_{\text{ref}}(x_o, y_o) \\ &+ \sum_{j=1}^N I_j f_j(x_o, y_o)] \delta(z_o - d) \\ &+ I_a \vec{J}_a(x_o, y_o, z_o) \end{aligned} \quad (7)$$

where $\vec{J}_a(x_o, y_o, z_o)$ is the attachment mode, and J_{ax} , J_{ay} , and J_{az} are defined in (3), (5), and (6), respectively. The f_j piecewise sinusoidal (PWS) expansion functions and J_{inc} and J_{ref} represent traveling waves of the fundamental microstrip mode as in [12]. The I_1 , I_2 , \dots , I_N , and I_a are the unknown coefficients of the current expansion modes.

To satisfy the boundary condition on the line, we have

$$[Z] = \begin{bmatrix} Z_{11} & \cdots & Z_{1N} & (-Z_{1c} + jZ_{1s}) & Z_{1a} \\ Z_{21} & \cdots & Z_{2N} & (-Z_{2c} + jZ_{2s}) & Z_{2a} \\ \vdots & \vdots & \vdots & \vdots & \vdots \\ Z_{N+1,1} & \cdots & Z_{N+1,N} & (-Z_{N+1,c} + jZ_{N+1,s}) & Z_{N+1,a} \\ Z_{a1} & \cdots & Z_{aN} & (-Z_{ac} + jZ_{as}) & Z_{aa} \end{bmatrix} \quad (11)$$

$$[I] = \begin{bmatrix} I_1 \\ I_2 \\ \vdots \\ I_N \\ R \\ I_a \end{bmatrix} \quad (12)$$

$$[V] = \begin{bmatrix} -Z_{1c} - jZ_{1s} \\ -Z_{2c} - jZ_{2s} \\ \vdots \\ -Z_{N+1,c} + jZ_{N+1,s} \\ -Z_{ac} - jZ_{as} \end{bmatrix}. \quad (13)$$

$$\begin{aligned} (1 - R) \vec{E}_c(x, y, d) + j(1 + R) \vec{E}_s(x, y, d) \\ + \sum_{j=1}^N I_j \vec{E}_j(x, y, d) + I_a \vec{E}_a(x, y, d) &= 0, \\ \text{on the line.} \end{aligned} \quad (8)$$

To satisfy the boundary condition on the pin, we have

$$\begin{aligned} (1 - R) \vec{E}_c(x_p, y_p, z) + j(1 + R) \vec{E}_s(x_p, y_p, z) \\ + \sum_{j=1}^N I_j \vec{E}_j(x_p, y_p, z) + I_a \vec{E}_a(x_p, y_p, z) &= 0, \\ \text{on the pin.} \end{aligned} \quad (9)$$

Now, we have a pair of equations with $N + 2$ unknowns. These unknowns are the complex amplitudes of the N PWS modes, the attachment mode and the complex voltage reflection coefficient. The moment method is used to discretize the EFIE's into a matrix equation for the $N + 2$ unknowns. PWS functions were chosen as the first $N + 1$ testing functions. The $N + 2$ testing function is a pulse function that exists on the pin. To account for the finite radius of the pin, a thin wire approximation is used as in [18].

Thus, we obtain a matrix equation for the unknown coefficients as

$$[Z][I] = [v] \quad (10)$$

where

$$[V] = \begin{bmatrix} -Z_{1c} - jZ_{1s} \\ -Z_{2c} - jZ_{2s} \\ \vdots \\ -Z_{N+1,c} + jZ_{N+1,s} \\ -Z_{ac} - jZ_{as} \end{bmatrix}. \quad (13)$$

For further details, readers can refer to [12] and [20].

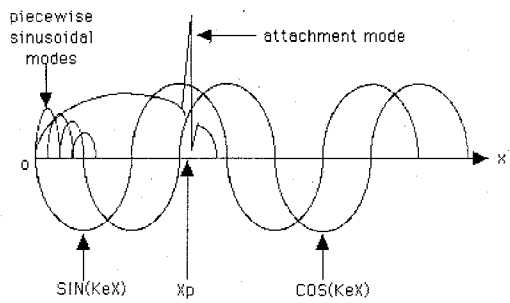


Fig. 2. Current distribution of the basis functions.

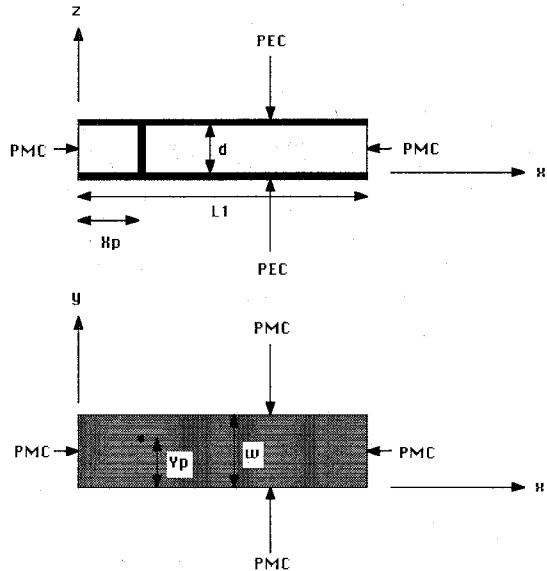


Fig. 3. Equivalent model for generating the attachment mode.

A computer program has been written to evaluate the impedance matrix and voltage vector elements, and to solve for the coefficients of the current expansion modes and the voltage reflection coefficient.

III. RESULTS

In order to verify the theory discussed above, several experiments were performed and the results compared to theory. For general purpose applications, we choose the width of the microstrip line such that its characteristic impedance is about 50Ω . This width becomes electrically large at higher frequencies. Because of this, we expect higher error will occur at higher frequencies since our model ignores y -directed current on the line, which become increasingly important as the line width becomes electrically larger. We also need to identify possible sources of measurement error in order to improve the measurement accuracy. One possible source of error is the discontinuity which exists due to the transition from coaxial cable connector to the microstrip line. In the theoretical treatment, it is assumed that the source is located at infinity, and a traveling wave with the fundamental mode effective propagation constant is incident upon the discontinuity. In reality, we have a limitation on the length of the line due to our spinner size. However, we can use

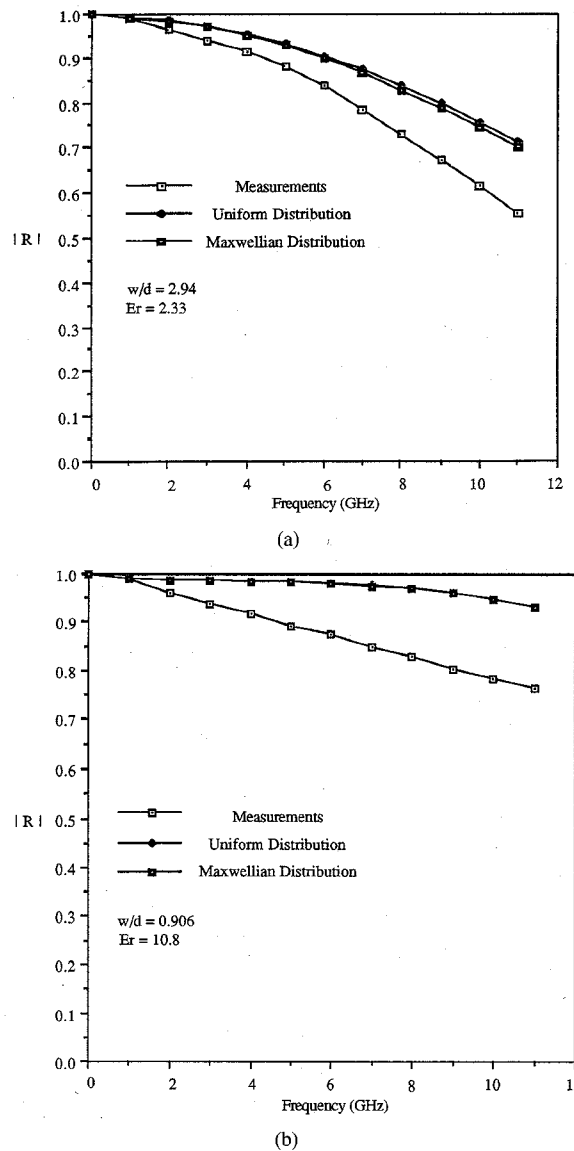


Fig. 4. Reflection coefficient magnitude of an open-end microstrip line.

the time-gating feature of the HP-8510 vector network analyzer which involves numerically transforming from frequency-domain to time-domain to remove the effect of the discontinuity. Using this technique, we obtain good results for line lengths longer than about 12 cm. We also measure over a 11 GHz bandwidth to insure good results using the time-gating technique.

Fig. 4(a) and (b) shows the calculated and measured data for two open-end microstrip lines. The open-end model is based on the one used in [12] which assumes that only x -directed current exists on the microstrip line. As can be seen, the error can be as high as 20% at higher frequencies.

Fig. 5 shows comparison of the measured reflection coefficient magnitude between an open-end and open-end with the shorting pin microstrip lines. One difference between them is that a resonant behavior is observed. At lower frequencies, radiation from the open-end is not very significant. Thus, two curves stay close to each other. However, at higher frequencies, radiation from the open-

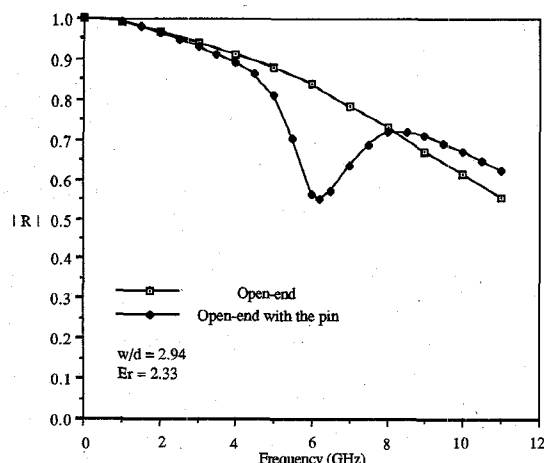


Fig. 5. Comparison of the measured reflection coefficient magnitude between open-end and open-end with shorting pin microstrip lines.

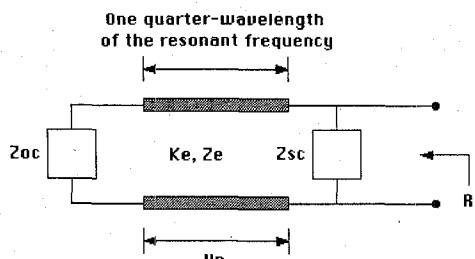


Fig. 6. Equivalent transmission line circuit of the resonant phenomenon.

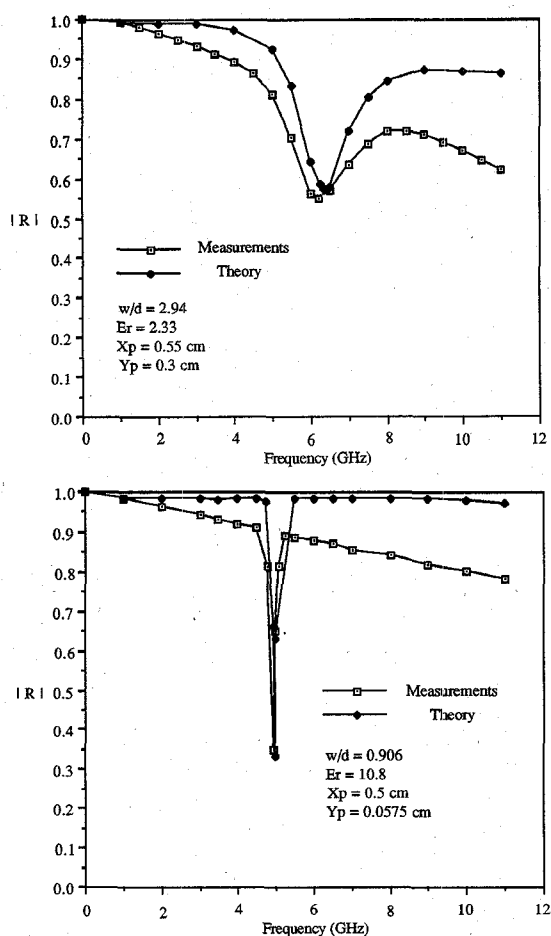


Fig. 7. Comparison between the calculated and measured reflection coefficient magnitude of an open-end microstrip line with a shorting pin.

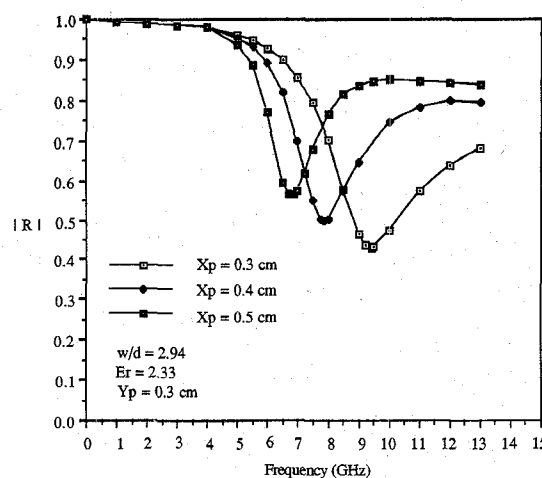


Fig. 8. Calculated reflection coefficient magnitude for different pin position.

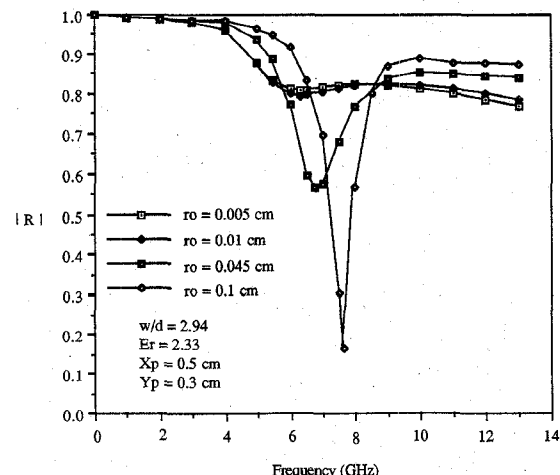


Fig. 9. Calculated reflection coefficient magnitude for different pin radii.

end becomes more significant. Some power is reflected by the shorting pin before it reaches the open-end. Thus, more power is reflected back to the source and the reflection coefficient magnitude is greater.

Fig. 6 shows an equivalent transmission line circuit which can be used to explain the resonant phenomenon. With one end open and the other end partially shorted, a quarter wavelength resonator is formed. By using the effective propagation constant at the resonant frequency to calculate the quarter wavelength distance, we can confirm the above idea.

Fig. 7(a) and (b) shows comparison of the reflection coefficient magnitude between an open-end microstrip line with a shorting pin and measurements. The model accurately describes the resonant behavior near the open-end. But, due to the neglect of the y -directed current component, we have a result where the error can be as high as 30% at higher frequencies.

Fig. 8 shows the calculated reflection coefficient magnitude of the open-end with the shorting pin for different pin position. The resonant frequency moves to higher frequency and the resonant bandwidth becomes larger when the pin position is moved closer to the open-end. The result is reasonable because the closer the pin position is to

the open-end, the smaller the effective resonant frequency quarter-wavelength. Thus, there is more radiation from the open-end.

Fig. 9 shows the calculated reflection coefficient magnitude of the open-end with the shorting pin for different pin radii. As the pin radius increases, the quarter-wavelength resonator has a higher Q and the resonant bandwidth becomes smaller. Also, because the effective quarter-wavelength becomes smaller, the resonant frequency increases. When the pin radius is very small, the resonant phenomenon becomes insignificant, and the structure acts like an open-end.

IV. CONCLUSION

A full-wave analysis has been presented for the problem of open-end microstrip line terminated with a shorting pin. We have been able to obtain a good approximation for this complicated problem and give some direction for future research. The author has written an efficient

candidate of this error. For example, no attempt was made to model ohmic losses due to the finite conductivity of the conductors, or the surface wave radiation at the substrate edge due to the finite substrate and ground plane [19]. In addition, the assumption of uniform current on the pin limits accuracy as the substrate gets electrically thicker at higher frequencies.

By including the y -directed current component in our model, we introduce more unknown current expansion mode coefficients, and as a result, a new set of testing function is required to discretize the integral equation. Since the complexity has increased, the computational efficiency may be significantly decreased. Thus, more effort on reducing the computation time is necessary in future research.

APPENDIX

(A1) through (A3) define the spectral domain Green's function for an infinitesimal x -directed current source:

$$G_{xx}(k_x, k_y, z | d) = \frac{-jZ_o(\epsilon_r k_0^2 - k_x^2) k_2 \cos(k_1 d) + jk_1(k_o^2 - k_x^2) \sin(k_1 d)}{T_e T_m} \sin(k_1 z) \quad (A1)$$

$$G_{yx}(k_x, k_y, z | d) = \frac{jZ_o}{k_o} \frac{k_x k_y [k_2 \cos(k_1 d) + jk_1 \sin(k_1 d)]}{T_e T_m} \sin(k_1 z) \quad (A2)$$

$$G_{zx}(k_x, k_y, z | d) = \frac{Z_o}{k_o} \frac{k_x k_2 \cos(k_1 z)}{T_m}. \quad (A3)$$

(A4) through (A6) define the spectral domain Green's function for an infinitesimal y -directed current source:

$$G_{xy}(k_x, k_y, z | d) = \frac{jZ_o}{k_o} \frac{k_x k_y [k_2 \cos(k_1 d) + jk_1 \sin(k_1 d)]}{T_e T_m} \sin(k_1 z) \quad (A4)$$

$$G_{yy}(k_x, k_y, z | d) = \frac{-jZ_o}{k_o} \frac{(\epsilon_r k_o^2 - k_y^2) k_2 \cos(k_1 d) + jk_1(k_o^2 - k_y^2) \sin(k_1 d)}{T_e T_m} \sin(k_1 z) \quad (A5)$$

$$G_{zy}(k_x, k_y, z | d) = \frac{Z_o}{k_o} \frac{k_y k_2 \cos(k_1 z)}{T_m}. \quad (A6)$$

program to calculate the theoretical results. The typical running time for a single frequency on a CRAY X-MP/18se supercomputer is about 200 s. For the open-end, the reflection coefficient magnitude has been calculated using the theory of [12] and compared with the measured data. The error can be as large as 20% at higher frequencies. The reason for this error is probably that y -directed current components are neglected. While this approximation is valid for electrically narrow lines, it becomes increasingly crude as the electrical width of the line increases. For the open-end with the shorting pin, the reflection coefficient magnitude also has been calculated and compared with the measured data. The error can be as large as 30% at higher frequencies. Since we have considered x -, y -, and z -directed current components in our attachment mode model, the resonant behavior is accurately described by this model. Thus, we expect that most of the error is coming from ignoring the contribution of the y -directed current. However, some other factors can also be the possi-

(A7) through (A9) define the spectral domain Green's function for an infinitesimal z -directed current source:

$$G_{xz}(k_x, k_y, d | z_o \leq d) = \frac{-Z_o}{k_o} \frac{k_x k_2 \cos(k_1 z_o)}{T_m} \quad (A7)$$

$$G_{yz}(k_x, k_y, d | z_o \leq d) = \frac{-Z_o}{k_o} \frac{k_y k_2 \cos(k_1 z_o)}{T_m}. \quad (A8)$$

$$G_{zz}(k_x, k_y, z \leq d | z_o \leq d)$$

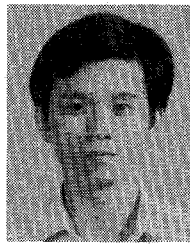
$$= \begin{cases} -\delta(z - z_o) + \frac{\beta^2 \cos(k_1 z)}{k_1 T_m} \\ \cdot \{ \epsilon_r k_2 \sin[k_1(d - z_o)] \\ - jk_1 \cos[k_1(d - z_o)] \}, & 0 \leq z \leq z_o \\ \frac{\beta^2 \cos(k_1 z_o)}{k_1 T_m} \{ \epsilon_r k_2 \sin[k_1(d - z)] \\ - jk_1 \cos[k_1(d - z)] \}, & z_o < z \leq d \end{cases} \quad (A9)$$

ACKNOWLEDGMENT

The authors would like to thank Dr. E. A. El-Sharway of Arizona State University for his helpful suggestions regarding this research.

REFERENCES

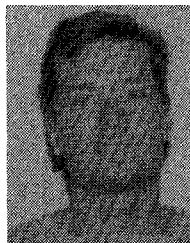
- [1] I. Wolff, G. Kompa, and R. Mehran, "Calculation method for microstrip discontinuities and T-junctions," *Electron. Lett.*, vol. 8, pp. 177-179, 1972.
- [2] G. Kompa and R. Mehran, "Planar waveguide model for calculating microstrip components," *Electron. Lett.*, vol. 11, pp. 459-460, 1975.
- [3] W. Menzel and I. Wolff, "A method for calculating the frequency-dependent properties of microstrip discontinuities," *IEEE Trans. Microwave Theory Tech.*, vol. MTT-25, pp. 107-112, 1977.
- [4] X. Zhang, J. Fang, K. K. Mei, and Y. Liu, "Calculations of the dispersive characteristics of microstrips by the time-domain finite difference method," *IEEE Trans. Microwave Theory Tech.*, vol. 36, pp. 263-267, 1988.
- [5] T. Shibata, T. Hayashi, and T. Kimura, "Analysis of microstrip circuits using three-dimensional full-wave electromagnetic field analysis in the time-domain," *IEEE Trans. Microwave Theory Tech.*, vol. 36, pp. 1064-1070, 1988.
- [6] X. Zhang and K. K. Mei, "Time-domain finite difference approach to the calculation of the frequency-dependent characteristics of microstrip discontinuities," *IEEE Trans. Microwave Theory Tech.*, vol. 36, pp. 1775-1787, 1988.
- [7] W. Pascher and R. Pregla, "Full-wave analysis of complex planar microwave structures," *Radio Science*, vol. 22, pp. 999-1002, 1987.
- [8] S. Nam, H. Ling, T. Itoh, "Time-domain method of lines applied to planar guided wave structures," *IEEE Trans. Microwave Theory Tech.*, vol. 37, pp. 897-901, 1989.
- [9] J. R. James and A. Henderson, "High-frequency behaviour of microstrip open-circuit terminations," *IEE J. Microwaves, Optics and Acoustics*, vol. 3, pp. 205-218, 1979.
- [10] R. H. Jansen, "Hybrid mode analysis of end effects of planar microwave and millimeterwave transmission lines," *Proc. Inst. Elec. Eng.*, vol. 128, pt. H, pp. 77-86, 1981.
- [11] P. B. Katehi and N. G. Alexopoulos, "Frequency-dependent characteristics of microstrip discontinuities in millimeter-wave integrated circuits," *IEEE Trans. Microwave Theory Tech.*, vol. MTT-33, pp. 1029-1035, 1985.
- [12] R. W. Jackson and D. M. Pozar, "Full-wave analysis of microstrip open-end and gap discontinuities," *IEEE Trans. Microwave Theory Tech.*, vol. MTT-33, pp. 1036-1042, 1985.
- [13] J. R. Mosig, "Arbitrarily shaped microstrip structures and their analysis with a mixed potential integral equation," *IEEE Trans. Microwave Theory Tech.*, vol. MTT-36, pp. 314-323, 1988.
- [14] L. P. Dunleavy and P. B. Katehi, "A generalized method for analyzing shielded thin microstrip discontinuities," *IEEE Trans. Microwave Theory Tech.*, vol. 36, pp. 1758-1766, 1988.
- [15] L. P. Dunleavy and P. B. Katehi, "Shielding effects in microstrip discontinuities," *IEEE Trans. Microwave Theory Tech.*, vol. 36, pp. 1767-1774, 1988.
- [16] R. W. Jackson, "Full-wave finite element analysis of irregular microstrip discontinuities," *IEEE Trans. Microwave Theory Tech.*, vol. 37, pp. 81-89, 1989.
- [17] T. Itoh, *Numerical Techniques for Microwave and Millimeter-wave Passive Structures*. New York: Wiley, 1989.
- [18] J. T. Aberle and D. M. Pozar, "Analysis of infinite arrays of probe-fed rectangular microstrip patches using a rigorous freed model," *Proc. Inst. Elec. Eng.*, vol. 136, pp. 110-119, 1989.
- [19] A. K. Bhattacharyya, "Effects of ground plane and dielectric truncations on the efficiency of a printed structure," *IEEE Trans. Antennas Propagat.*, vol. 39, pp. 303-308, 1991.
- [20] W. J. Tsay, "Analysis of a microstrip line terminated with a shorting pin," Master's thesis, Arizona State University, Tempe, 1991.



Wen-Jiunn Tsay was born in Hsinchu, Taiwan on July 26, 1960. He received the B.S. degree in electronic engineering from National Chiao Tung University, Hsinchu, Taiwan, in 1982 and the M.S. degree from Arizona State University, Tempe, Arizona, in 1991.

From 1982 to 1986, he served at the R.O.C. Army Headquarters and was the Deputy Commander of one electronic warfare company. From 1986 to 1988, he was with Microelectronics Technology Inc. as an R&D engineer, where he dedicated in the design of the Phase Locked Oscillator. In 1988, he joined the Telecommunications Research Center at Arizona State University as a graduate student. He was a Teaching Assistant and awarded ASU Graduate Academic Scholarship from 1989 to 1991. Currently a Ph.D. student at the University of Massachusetts at Amherst, his research interests include the application of the variational method analysis.

Mr. Tsay is a member of Phi Kappa Phi.



James T. Aberle received the B.S. and M.S. degrees in electrical engineering from Polytechnic Institute of New York (now Polytechnic University) in 1982 and 1985, respectively, and the Ph.D. degree in electrical engineering from the University of Massachusetts at Amherst in 1989.

From 1982 to 1985, he was employed by Hazeltine Corporation, Greenlawn, NY, where he worked on the development of wide-band phased arrays. He was a Graduate Research Assistant at the University of Massachusetts at Amherst from 1985 to 1989, where he developed and validated computer models for printed antennas. Currently an Assistant Professor at Arizona State University, his research and teaching interests are in the area of advanced electromagnetic techniques.

Dr. Aberle is a member of Eta Kappa NU, Tau Beta Pi and Sigma Xi.